Nanoscale

Accepted Manuscript

This article can be cited before page numbers have been issued, to do this please use: L. Zhang, R. Li, B. Tang and P. Wang, *Nanoscale*, 2016, DOI: 10.1039/C6NR03921A.

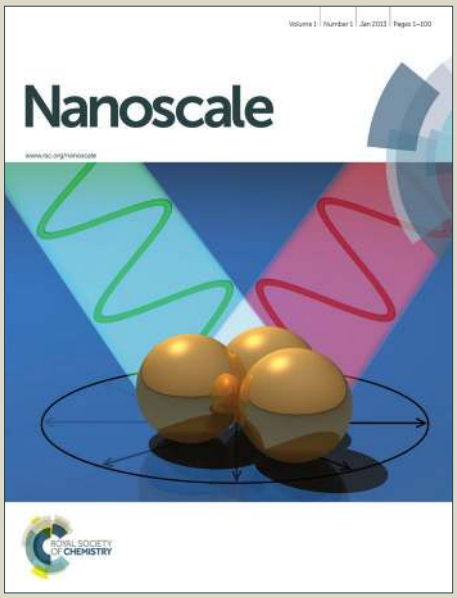

ROYAL SOCIETY OF CHEMISTRY

www.rsc.org/nanoscale

View Article Online
DOI: 10.1039/C6NR03921A

Solar-thermal conversion and thermal energy storage of graphene foam-based composite

Lianbin Zhang, Renyuan Li, Bo Tang and Peng Wang*

Water Desalination and Reuse Center, Division of Biological and Environmental Sciences and Engineering, King Abdullah University of Science and Technology, Thuwal 23955-6900, Saudi Arabia.

*Corresponding author e-mail: peng.wang@kaust.edu.sa

Abstract

Among various utilizations of solar energy, solar-thermal conversion has recently gained renewed research interest due to its extremely high energy efficiency. However, one limiting factor common to all solar-based energy conversion technologies is the intermittent nature of solar irradiation, which makes them unable to stand-alone to satisfy continuous energy need. Herein, we report a three-dimensional (3D) graphene foam and phase change material (PCM) composite for the seamlessly combined solar-thermal conversion and thermal storage for sustained energy release. The composite is obtained by infiltrating the 3D graphene foam with a commonly used PCM, paraffin wax. The high macroporosity and low density of the graphene foam allow for high weight fraction of the PCM to be incorporated, which enhances heat storage capacity of the composite. The interconnected graphene sheets in the composite provide (1) the solar-thermal conversion capability, (2) high thermal conductivity and (3) form stability of the composite. Under light irradiation, the composite effectively collects and converts the light energy into thermal energy, and the converted thermal energy is stored in the PCM and released in an elongated period of time

View Article Online
DOI: 10.1039/C6NR03921A

for sustained utilization. This study provides a promising route for sustainable utilization of solar energy.

Keywords: graphene; photothermal; thermal energy storage; phase change material; composite.

Introduction

Solar energy is the ultimate energy source of everything there is on the earth, and given its wide availability and inexhaustibility, solar energy is considered as the most renewable and clean energy source available to the mankind.[1-3] Tireless efforts have been made, especially in the past two decades, in efficient utilization of solar irradiation for energy and environmental gains.[4-11] Two typical examples are, photovoltaic (PV) materials, which convert solar irradiation to electricity,[4,5] and photocatalysis (PC) processes, which utilize solar energy to generate chemical fuels (e.g., hydrogen) or to treat contaminated water.[6-8] While popular, these processes face a common challenge of low energy conversion efficiencies, with generally the state-of-the-art PV system achieving <50% while that of PC < 5%.[5,8]

On the other hand, solar-thermal conversion in which photothermal materials are employed to harvest solar irradiation and convert it to heat as terminal energy for beneficial usage, a seemingly primitive and ancient means of utilizing solar energy, has gained renewed research interest in the past decade and found itself certain niche applications due to its operation simplicity and more importantly extremely high energy conversion efficiency.[9-18] In a sharp contrast to the PV and PC, with a proper design, including proper material selection and heat management, a modern solar-thermal conversion process can reach a perfect solar-to-heat conversion efficiency of almost 100%.[10] An emerging concept in solar-thermal conversion is localized interfacial heating for water distillation/evaporation, which has reached a total system energy efficiency >90% thus represents a new avenue for energy-efficient clean water production and wastewater treatment.[12-18]

Among energy-efficient photothermal materials are metallic nanoparticles (e.g., gold, silver, platinum), conjugated polymeric materials (e.g., polypyrrole, polyaniline), and carbon-based materials (e.g., carbon nanotubes, carbon black, graphite, graphene).[12-21] Graphene, an atom-thin layer of pure carbon, has distinguished itself among its peers owing to not only its high light absorption and photothermal efficiency but also its high thermal, electrical conductivity, and

View Article Online
DOI: 10.1039/C6NR03921A

superior mechanical strength.[22-25] Nevertheless, one limiting factor common to all solar-based energy conversion technologies is the intermittent nature of solar irradiation (i.e. low-insolation periods and nights), which makes them unable to stand-alone to satisfy continuous energy need. The solar-thermal conversion is no exception where proper thermal energy storage becomes essential to provide reliable and dispatchable thermal energy for sustainable utilization.

In general, current thermal energy storage methods are mainly twofold: sensible heat storage and latent heat storage.[10,26-28] Compared with the sensible heat storage, which involves storing thermal energy by raising the temperature of a solid or liquid and is highly dependent on the specific heat capacity of the material, the latent heat storage engages an isothermal process in which energy is stored during melting and released during freezing of a phase change material (PCM) and thus offers a much higher storage density and narrower temperature range therein.[26-33] Therefore, combining PCM-based heat storage with solar-thermal conversion can be a promising strategy in need. For such a composite to be effective, the following criteria with respect to its desirable thermophysical, kinetic and chemical properties should be met: (1) a high light-to-heat conversion efficiency of photothermal component and a high latent heat of PCM component, which necessitates a high weight fraction of the PCM in the composite; (2) a high thermal conductivity of the composite to allow for effective heat storing and releasing in the PCM; (3) a good chemical and structural stability of the composite in the course of the phase change (e.g., melting and freezing) to ensure the cyclic use of the material. With these considerations in mind, an interconnected macroporous and three-dimensional (3D) structure of a photothermal material with high thermal conductivity becomes a rational choice as a host of PCM.

In our previous study, we developed a facile *in situ* chemical reduction-assembly method to prepare 3D graphene foams, which exhibited 3D network structure of interconnected graphene sheets with low density, highly porous structures, and electrically conducting properties.[34] Because of the excellent photothermal effect of graphene, we believe that such a graphene foam would be an ideal scaffold to support PCMs. Herein, we report a graphene-PCM composite for the solar-thermal conversion and the thermal storage for sustained energy release. The composite was obtained by infiltrating the 3D graphene foam with a commonly used PCM, paraffin wax. The high macroporosity and low density of the graphene foam allow for high weight fraction of the PCM to be incorporated, which enhances heat storage capacity of the composite. The

View Article Online
DOI: 10.1039/C6NR03921A

interconnected graphene sheets in the composite provide (1) the solar-thermal conversion capability, (2) high thermal conductivity and (3) form stability of the composite. Under light irradiation, the composite effectively collects and converts the light energy into thermal energy, and the converted thermal energy is stored in the PCM and released in an elongated period of time for sustained utilization. In one further development, we employed the composite as a heat source for a thermoelectric device where the stored solar-generated thermal energy was utilized to generate sustained electricity when the solar irradiation was off.

Experimental

Materials

Graphite powder (<20 mm), sodium nitrate, potassium permanganate, hydrogen peroxide (30%), oxalic acid (OA), sodium iodide (NaI), ethanol, and paraffin wax were purchased from Sigma-Aldrich. All these chemicals were used as received. Deionized (DI) water purified in a Milli-Q (Millipore) system was used in all experiments.

Preparation of graphene foam

The graphene foams were prepared by an *in-situ* chemical reduction-induced self-assembly method reported previously.[34] Briefly, 20.0 mL of the graphene oxide (GO) suspension obtained by a modified Hummer's method with a concentration of 2.5 mg mL^{-1} was prepared, and then 0.5 g of OA and 1.0 g of NaI were added to the GO suspension to initiate GO reduction to reduced graphene oxide (rGO). The mixture was sonicated for 10 min and then transferred to an oil bath at 90°C for 12 hours without stirring. The resulted black cylinder of graphene (rGO) hydrogel was washed with ethanol and water in a Soxhlet extractor for 24 h to remove residual impurities and then the wet hydrogels were freeze-dried for 2 days to obtain graphene foams.

Preparation of graphene-wax composite

The graphene–wax composites were fabricated by infiltrating the previously prepared graphene foams (obtained from 2.5 mg mL^{-1} GO suspension) with liquid paraffin wax at 90°C as illustrated in Figure 1a. Due to the highly porous structure of the graphene foams and its oleophilicity, the molten wax quickly infiltrated into the foams, and the so-obtained composites were then cooled

View Article Online
DOI: 10.1039/C6NR03921A

down to room temperature. The mass fraction of wax in the composite was measured by comparing the weights of the foam before and after the wax infiltration, and at least three samples were measured to determine the average value. For the preparation of the simple mixture of graphene and wax, graphene powders obtained by the above mentioned reduction method were mixed with paraffin wax with a loading fraction of graphene ~3%, and the mixture was stirred continuously at 90ºC for 2 hours. Then the mixure was kept still at ambient condition to allow it to cool down to the room temperature to obtain the simple mixture of graphene and wax.

Characterizations

The morphology of the graphene foam and the composite was characterized by scanning electron microscopy (SEM) (FEI Company, Quanta 600). DSC data were obtained with a differential scanning calorimeter (Netzsch DSC 204 F1) with sealed Al pans. The amounts of the samples for the DSC measurements were around 10 mg and the measurements were conducted under N_2 flow with a heating and cooling rate of 5 $^{o}Cmin^{-1}$ in the range of 0-100ºC. Thermo-gravimetric analysis (TGA) of the samples was conducted on a Thermo-gravimetric Analyzer (Netzsch TG 209 F1) with a heating rate of 10 $^{o}Cmin^{-1}$. Diffuse reflectance spectra (DRS) were obtained by a UV-vis spectrophotometer (UV-2550, Shimadzu, Japan) with $BaSO_4$ as reflectance standard. The temperature and thermal images of the samples under the simulated solar light illumination were recorded by using a FLIR A655 infrared camera. The simulated solar irradiation was provided by a 150 W Oriel Solar Simulator. The output voltage was measured by a Keithley 2400 multimeter.

Results and discussion

The graphene foam was prepared following the *in situ* chemical reduction-induced self-assembly method previously developed in our group.[34] In the course of the graphene oxide (GO) reduction, the restored conjugated graphene structures allow for the strong interaction between separate reduced GO (rGO) nanosheets via the hydrophobic and π- π interactions, which enables the rGO to self-assemble into a stable monolithic graphene foam (Figure 1a).[34] The composite was obtained by simply infiltrating the graphene foam with hot liquid paraffin wax. Due to the highly porous structure of the graphene foam and its oleophilicity, the molten wax quickly infiltrated into the foam, and after the wax was cooled down to room temperature the graphene-wax composite could

View Article Online
DOI: 10.1039/C6NR03921A

be obtained. Scanning electronic microscopic (SEM) images in Figure 1b and 1c reveal the microscopic structure of the graphene foam and the composite. As can be seen, the graphene foam exhibited 3D network structures, having a large amount of interconnected and throughout pores with the pore sizes of 4.8±0.9 μm and with the pore walls of thin layers of stacked graphene sheets (Figure 1b). These interconnected pores allow for easy access by the liquid wax during the infiltration process. The SEM image in Figure 1c reveals that the wax infiltrated in and fully occupied the void space of the graphene foam and that the graphene sheets adhered well to the wax (inset of Figure 1c), presumably because of the good affinity between the hydrocarbon chain of the wax and the graphene sheets.

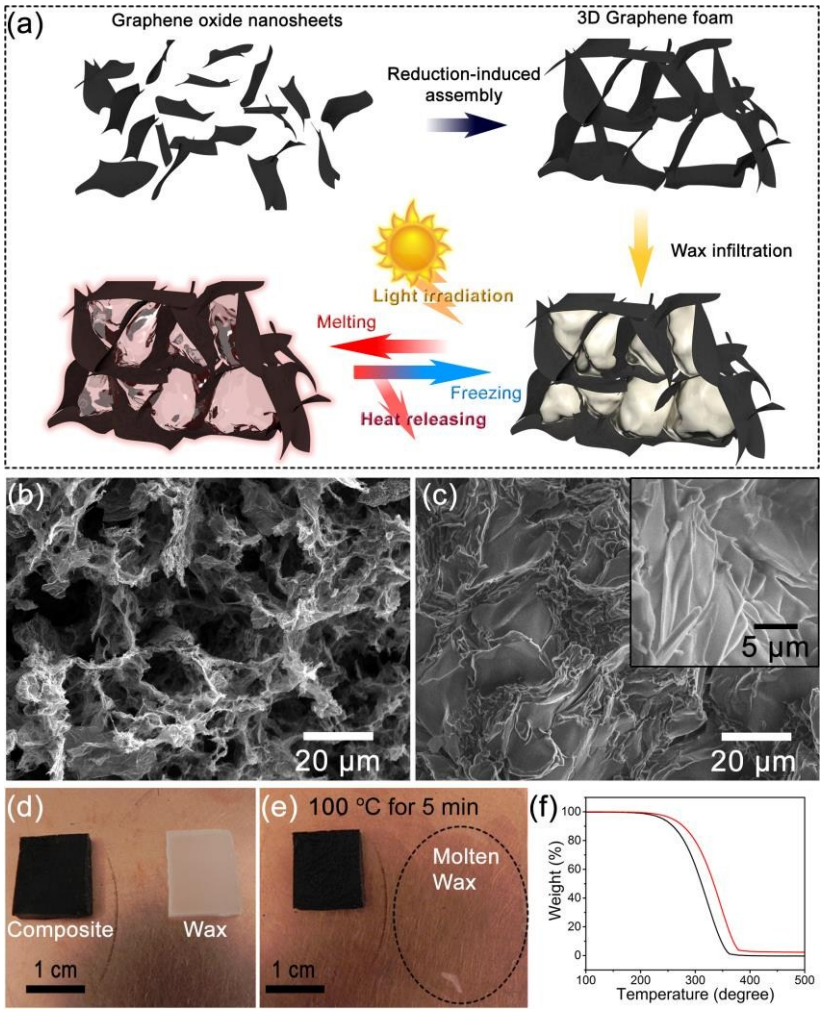

Figure 1. a) Schematic illustration for the preparation of the graphene foam and wax composite for the solar-thermal conversion and thermal energy storage. b) and c), SEM images of the graphene foam and the graphene-wax composite. Inset in (c): magnified view of the composite.

View Article Online
DOI: 10.1039/C6NR03921A

d) and e), digital photographs of the composite (left) and pristine wax (right: white sample) placed on a hot plate with a temperature of 100°C. f) TGA curves of the composite (red) and the pristine wax (black).

Due to the high porosity, the pristine graphene foam exhibited a low density of ~12.3 mg cm^{-3} and, after the wax infiltration, the composite had a high mass fraction of wax (97.8±0.2%), which was measured by comparing the weights of the foam before and after the wax infiltration. It is worth mentioning that the capillary effect between the graphene foam and the liquid wax resulted in a volume shrinkage of ~25.5% of the composite after the infiltration and the solidification of the wax. We believe that the capillary effect is conducive in confining the wax in pores of the graphene foam and in effectively preventing the liquid wax from leaking at elevated temperature (i.e., above the melting point of the wax), which is critical to the form-stability of the composite. When placed on a hot plate with a temperature of 100°C for 30 minutes, the composite maintained its original shape, without significant form-distortion and resulting in no leak of the liquid wax while, in a sharp contrast, the pristine wax pellet (i.e., without the graphene foam scaffold) quickly melted into liquid within 5 minutes under otherwise the same conditions (Figure 1d and e). Similarly, it was also found that a simple mixture of the graphene and wax with the same weight ratio (i.e., no 3D foam structure of graphene) melted into liquid and deformed at elevated temperature (ESI, Figure S1). The comparisons convincingly prove the critical role of the 3D graphene foam, even though its small weight percentage (<3.0%), in maintaining the form-stability of the resultant composite.

Thermal stability of the composite was examined by using a thermogravimetric analysis (TGA) whose results are presented in Figure 1f. Compared with the pristine wax, the composite had a higher decomposition temperature (~348°C vs. ~322°C), indicating the interaction between the wax and the graphene and more importantly improved thermal stability of the composite. Besides, the wax weight fraction of the composite estimated from the TGA (97.8%) agreed well with the one obtained from the weighing measurement.

Graphene is well known to have strong light absorbing capability.[13,25] To evaluate the light absorbing capability of the composite, diffuse reflectance spectra of the composite were measured and the light reflection results are presented in Figure 2a. Clearly, compared with the pristine wax,

View Article Online
DOI: 10.1039/C6NR03921A

both the graphene foam and the composite with a thickness of ~ 1.0 mm exhibited low light reflection (less than 2.5%) within a wide wavelength range (i.e., 200-800 nm) (Figure 2a) and zero transmittance (ESI, Figure S2), demonstrating strong light absorbance by the graphene. The absorbed light was converted to heat by the graphene. To study the solar-thermal conversion and thermal energy storage performances of the materials, samples of the composite, pristine wax, and graphene foam were irradiated by the simulated solar light, and an infrared (IR) camera was used to capture thermal images and to record the temperature change of the samples in air, as schematically presented in Figure 2b. To minimize the heat loss, three circular non-through holes were made on surface of a thermally insulating polystyrene foam and the samples with the same weight of ~0.2 g were placed in these holes whose sizes were identical to those of samples. The simulated solar light was shined on top of the samples. All sample had the same top surface area of ~0.246 cm^2 exposed to the light and the measurement was conducted at constant ambient temperature (~22°C). Under the light irradiation, a steady-state temperature, which is defined as the temperature at which the heat generation under light irradiation and heat dissipation due to radiative heat flux is at equilibrium, would be established. Figure 2c shows the steady-state temperature of the samples as a function of varying light intensity and it can be seen that the steady-state temperature of all the samples increased with increasing light intensity. For instance, under 1500Wm^{-2} light irradiation, the steady-state temperature of the graphene foam, composite, and the pristine wax were 76.9, 66.7, and 40.7°C, respectively, with the graphene foam and the composite showing a much faster temperature rise to their steady-state points than the pristine wax (Figure 2d and e). These results demonstrate the strong light-to-heat conversion capability of the graphene.

View Article Online
DOI: 10.1039/C6NR03921A

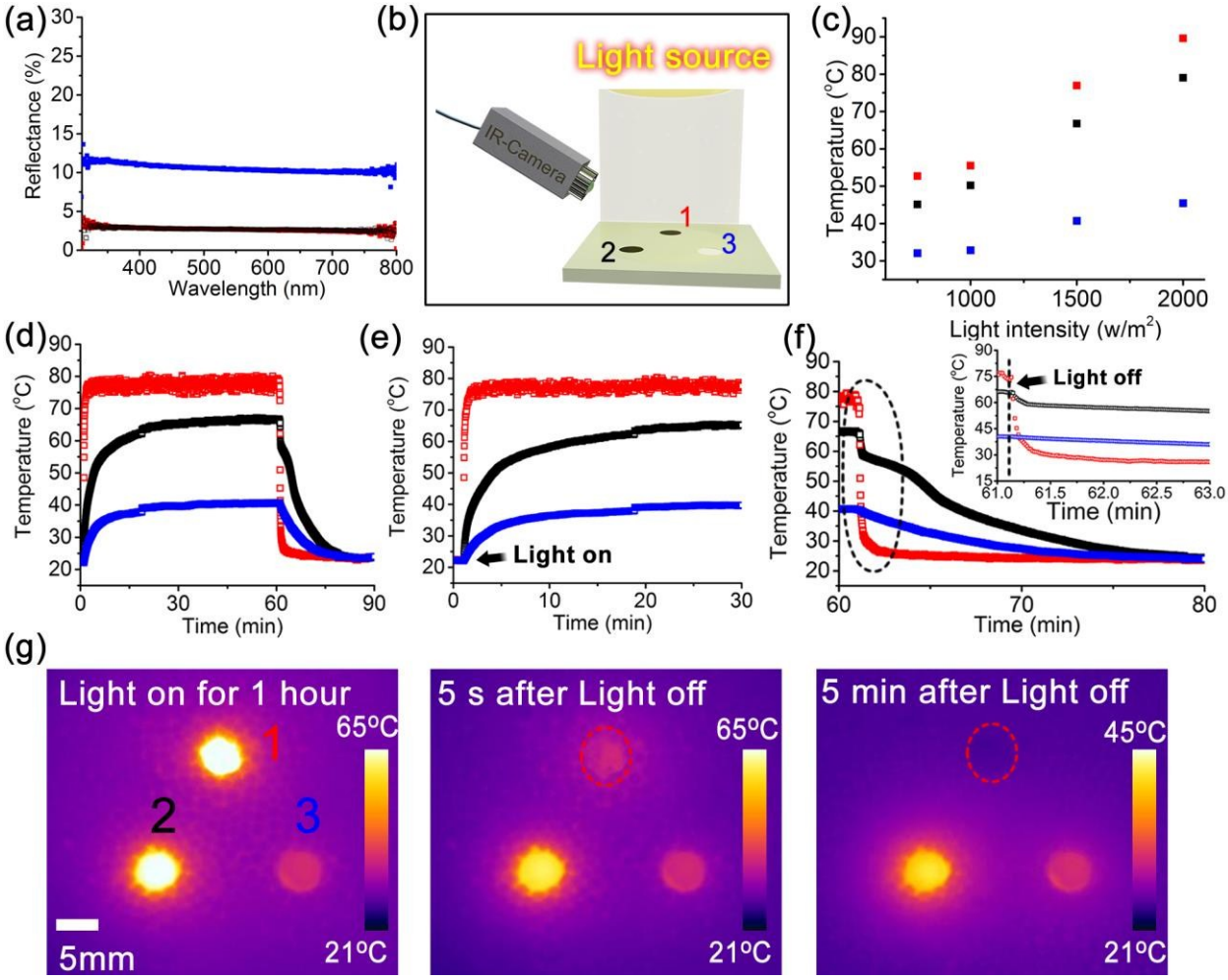

Figure 2. a) Diffuse reflectance spectra of the graphene foam (red), composite (black), and wax (blue). The reflectance of the composite was similar to that of the graphene foam, leading to the overlap of these two curves. b) Schematic illustration of the photothermal performance measurement setup of the samples. **1**: graphene foam; **2**: composite; **3**: pristine wax. The pellet samples of the graphene foam, composite and wax were inserted in thermally insulating polystyrene foam board, and the surfaces of these samples with the same surface area were exposed to the simulated solar light. An IR camera was used to capture the thermal image of the samples. c) The steady-state temperatures of graphene foam (red), composite (black), and pristine wax (blue) in air, under light irradiation with different light intensity. d) Time-course of the sample temperature under solar light irradiation (1500 Wm^{-2}). e) and f), Details of the temperature change in heating and cooling processes in (d). Inset in (f) shows the details of the outlined parts. Arrows in (e) and (f) indicate the time when the light was turned on and off during the measurements. g) Thermal images of the samples under the light irradiation for 1 hour (left panel), 5 seconds after the light was turned off (middle panel), and 5 min after the light off (right panel). **1**: graphene foam; **2**: composite; **3**: pristine wax. Outlines in the middle and right panels indicate the location of the graphene foam.

View Article Online
DOI: 10.1039/C6NR03921A

The fast temperature equilibration of the composite under the light irradiation can also be attributed to its thermal conductivity, which is an important parameter of the solar-thermal conversion and thermal storage composite. The thermal conductivity of the composite was estimated to be 0.617 $Wm^{-1}K^{-1}$ by IR thermal imaging (The measurement details can be found in ESI part, Figure S3) while that of the pristine wax was only ~0.309 $Wm^{-1}K^{-1}$. We believe that the good contact between the graphene sheets and the paraffin wax in the composite enables the composite to inherit the high thermal conductivity from individual graphene sheets[35] and it is the 3D network of the interconnected graphene sheets in the foam that provides dominant heat transfer pathways.[29,36] Thus, it is not a surprise that the simple mixture of graphene and wax composite (i.e., without 3D interconnected foam structure of graphene) with the same weight fraction only achieved a thermal conductivity of ~0.372 $Wm^{-1}K^{-1}$. It should be noted that the relatively low thermal conductivity of the graphene-wax composite in this study, compared with those of chemical-vapor-deposition produced graphene and compressed expanded natural graphite based composites,[29,36] was probably because of the low loading fraction of and the defects in the chemically reduced graphene oxide.

By design, the composite is expected to effectively collect, convert the light irradiation into heat, and at the same time store the thermal energy. To prove the energy storage capability of the composite, the light was turned off after one-hour irradiation and the temperature decline curves of the samples were recorded (Figure 2d and f). A temperature plateau could be clearly observed during the cooling of the composite, which is an expected result of stored heat releasing by a PCM. The same phenomenon was not observed on the graphene foam, which quickly cooled down to ambient temperature also as shown in the thermal images of Figure 2g. These results indicate that the combination of the photothermal graphene and the PCM is essential for the successful solar-thermal conversion and thermal energy storage.

It is the wax that imparts the composite with the shown thermal storage capability. The thermophysical properties of the wax were then investigated by differential scanning calorimetric (DSC) measurement and were compared with those of the pristine wax. Figure 3a presents the DSC curves of the composite and the pristine wax undergoing melting and freezing cycles and Table 1 summarizes their thermal characteristics. As revealed by the DSC measurements in Figure 3a, the composite and the pristine wax exhibited quite similar endothermic and exothermic

View Article Online
DOI: 10.1039/C6NR03921A

behaviors. It can be seen that the melting point (T_m) and freezing point (T_f) (peak temperature of the DSC curves) of the pristine wax and the composite were quite close, indicating that the infiltration of the wax in the graphene foam had little effect on its thermal properties. From the DSC endothermic curve of the composite, it can be seen that the melting took place over a wide temperature range, starting at ~31°C and ending at ~66°C. While for the freezing of the composite, a temperature range between 58°C and 26°C was observed. The melting (ΔH_m) and freezing (ΔH_f) enthalpy of the composite calculated from the DSC curves was only slightly lower than that of the pristine wax, which was a result of the high wax fraction in the composite. Such a high loading fraction of the PCM in the composite allows for high heat storage capacity. Under the light irradiation, the incident light is absorbed by the graphene in the composite and at the same time converted to heat, which leads to a temperature increase of the composite and phase change (melting) of the wax in the composite, storing the thermal energy in the composite (Figure 2d and e). The solar-thermal energy storage efficiency (Ƞ) of the composite under the light irradiation was estimated by the ratio between the stored thermal energy and the received light energy using equation (1):

$$\eta = \frac{Qs}{Q} = \frac{m \times \Delta H}{P \times A \times t} \qquad (1)$$

Where, Qs is the stored thermal energy by the composite, Q is the received light energy by the composite, m (~0.2 g) is the mass of the composite sample, P is the intensity of the simulated solar light, A (0.246 cm^2) is the surface area of the composite exposed to the light, t is the duration of light irradiation for heating the composite from a lower temperature (T1) to a higher temperature (T2), and ΔH is enthalpy change of the composite between the temperature range (T1-T2) and can be obtained by the DSC measurements. Under the simulated solar irradiation with a light intensity of 1500 Wm^{-2}, for example, when the temperature of the composite increased to 60°C from 30°C, which corresponded to an enthalpy change (ΔH) of 100 Jg^{-1}, a storage efficiency (Ƞ) was calculated to be 79.9% for this period.

View Article Online
DOI: 10.1039/C6NR03921A

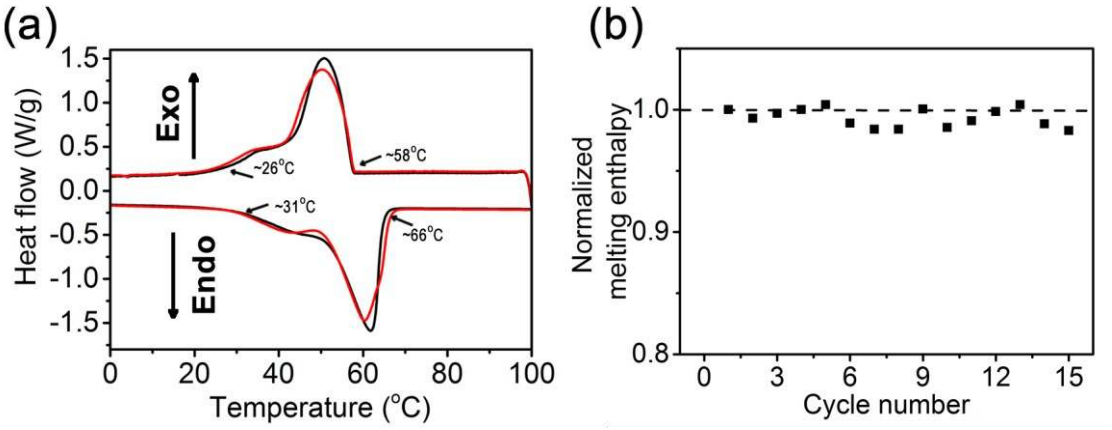

Figure 3. a) DSC curves of the graphene-wax composite (red) and the pristine wax (black). b) Normalized melting enthalpy of the composite during 15 cycles of melting and freezing processes.

Table 1. Thermophysical properties of the wax and the graphene-wax composite.

	T_m (°C)	T_f (°C)	ΔH_m (J/g)	ΔH_f (J/g)
Pristine wax	61.8	50.8	203	199
Composite	60.8	49.1	200	197

Upon the removal of the light, a temperature plateau could be observed during the cooling process of the composite starting at ~58°C (Figure 2f), corresponding to the thermal energy releasing characteristic of phase change (freezing) of the wax in the composite. In addition, the composite exhibited a very good thermal stability. We found that during 15 melting-freezing cycles, the melting enthalpy of the composite showed negligible change, which promises for repeated uses of the composite (Figure 3b).

With the combined solar-thermal conversion and thermal energy storage capability, the graphene-wax composite can be expected as heat source for solar thermoelectric generator for sustained power generation. As a proof of concept, we designed a solar-driven thermoelectric conversion system to demonstrate sustained power generation by the composite (Figure 4a). In more details, the composite was fixed on the hot end of a commercially available thermoelectric conversion module (4.0 cm×4.0 cm) and was exposed to the simulated solar irradiation, and the

View Article Online
DOI: 10.1039/C6NR03921A

cold end of the module was attached to an aluminum bulk with cooling fans as heat sink. A digital voltage meter was used to measure the open-circuit voltage of the thermoelectric module. As a control, the thermoelectric module in the absence of the composite generated maximum voltages of 0.09 and 0.13 V under the light intensity of 1000 and 1500 Wm^{-2}, respectively and the output voltages quickly dropped to less than 0.01V within ~100 seconds once the light was turned off (Figure 4b). As expected, significantly improved voltages (0.16 and 0.21 V) were obtained on the thermoelectric module with the composite under otherwise the same experimental conditions (Figure 4c). Most importantly, a unique feature of the composite integrated thermoelectric module lied in its prolonged thermal response, which was a result of the heat storage by the composite and which enabled the continuation of the voltage output even when the light was off. As shown in Figure 4d, the time for the voltage drop to 0.01V on the device with the composite was about 12 minutes. As a demonstration of a practical application of the composite, the thermoelectric module with the composite (~13.5 g) was exposed first under light irradiation (1500 Wm^{-2}) for 60 minutes and then was used to power an electronic fan with the light off (Figure 4e). It was observed that a constant fan rotation continued for 10 minutes in the absence of light. This feature of the sustained electricity generation by the composite-integrated thermoelectric device could be useful as it provides a buffer mechanism against the influence by temporary blocking of incident light, reducing power fluctuations.

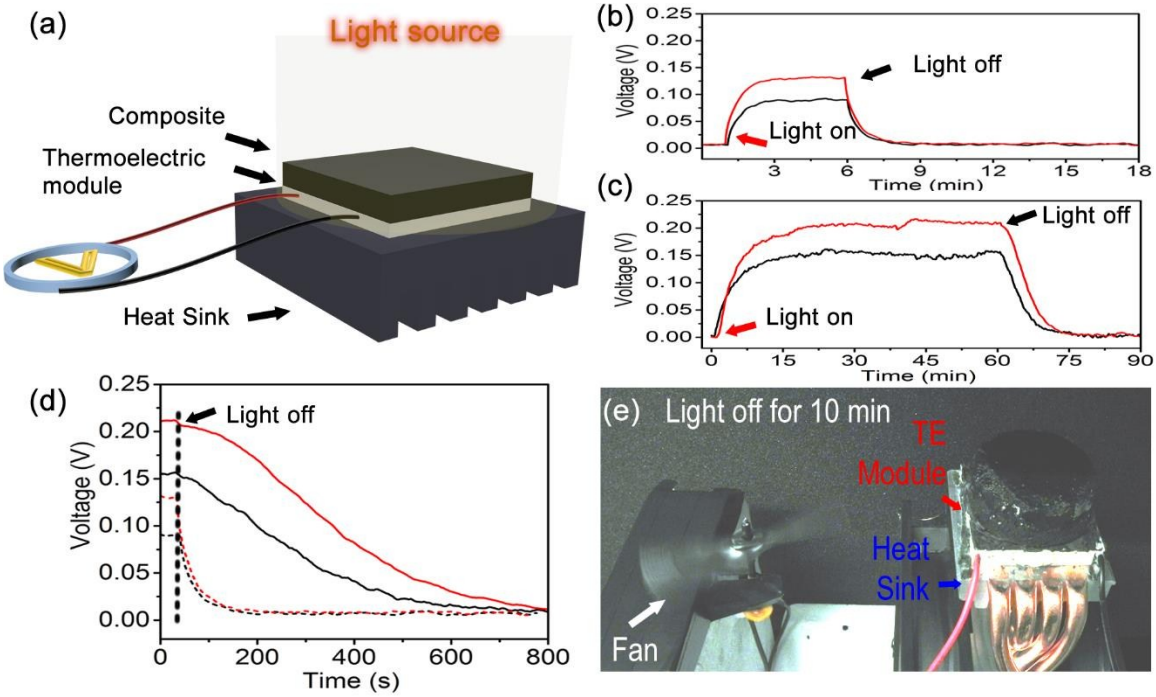

View Article Online
DOI: 10.1039/C6NR03921A

Figure 4. a) Schematic illustration of the solar thermoelectric device based on graphene-wax composite. b) and c), Time-course of the open-circuit voltage of the thermoelectric modules under the simulated solar light irradiations. red curve: 1500 Wm^{-2}; black: 1000 Wm^{-2}. b: without composite; c: with composite (6.3g). d) Time course of voltage decay of the thermoelectric modules with (solid lines) and without the composite (dash lines) on the hot end of the module after the light was turned off. red curve: 1500 Wm^{-2}; black: 1000 Wm^{-2}. e) Digital photograph showing continuous rotation of the electronic fan driven by the thermoelectric device with 13.5 g composite on the hot end after the light was off.

Conclusions

In this study, we rationally devised and fabricated a novel composite of graphene-wax for the combined purpose of solar-thermal conversion and thermal energy storage. The composite was prepared by infiltrating the self-assembled 3D graphene foams with phase change material of paraffin wax. Under the light irradiation, the composite effectively collects and converts the light energy into thermal energy, and the converted thermal energy is stored in the PCM and released, when the light is off, for an elongated period of time for sustained utilization. We believe that this study provides a promising route for sustainable utilization of solar energy.

Acknowledgments

The research reported in this publication was supported by funding from King Abdullah University of Science and Technology (KAUST) CRG-3.

Electronic supplementary information (ESI) available.

References

1. N. S. Lewis and D. G. Nocera, *Proc. Natl. Acad. Sci. USA*, 2006, **103**, 15729-15735.
2. G. W. Crabtree and N. S. Lewis, *Phys. Today*, 2007, **60**, 37-42.
3. N. S. Lewis, *Science*, 2007, **315**, 798-801.
4. M. Grätzel, *Nature*, 2001, **414**, 338-344.
5. T. M. Razykov, C. S. Ferekides, D. Morel, E. Stefanakos, H. S. Ullal and H. M. Upadhyaya, *Sol. Energy*, 2011, **85**, 1580-1608.

View Article Online
DOI: 10.1039/C6NR03921A

6. P. V. Kamat, *J. Phys. Chem. C*, 2007, **111**, 2834-2860.

7. M. Ni, M. K. H. Leung, D. Y. C. Leung and K. Sumathy, *Renew. Sustain. Energy Rev.*, 2007, **11**, 401-425.

8. H. Tong, S. Ouyang, Y. Bi, N. Umezawa, M. Oshikiri and J. Ye, *Adv. Mater.*, 2012, **24**, 229-251.

9. T. P. Otanicar, P. E. Phelan, R. S. Prasher, G. Rosengarten and R. A. Taylor, *J. Renew. Sustain. Energy*, 2010, **2**, 033102.

10. L. A. Weinstein, J. Loomis, B. Bhatia, D. M. Bierman, E. N. Wang and G. Chen, *Chem. Rev.*, 2015, **115**, 12797-12838.

11. P. Phelan, R. Taylor, R. Adrian, R. Prasher and T. Otanicar, in *Nanoparticle Heat Transfer and Fluid Flow* (Eds: W. J. Minkowycz, E. M. Sparrow and J. Abraham), CRC Press, Boca Raton, FL, USA 2012, pp. 123–142.

12. Y. Wang, L. B. Zhang and P. Wang, *ACS Sustainable Chem. Eng.*, 2016, **4**, 1223-1230.

13. Y. Ito, Y. Tanabe, J. Han, T. Fujita, K. Tanigaki and M. Chen, *Adv. Mater.*, 2015, **27**, 4302-4307.

14. G. Ni, N. Miljkovic, H. Ghasemi, X. Huang, S. V. Boriskina, C.-T. Lin, J. Wang, Y. Xu, Md. M. Rahman, T. Zhang and G. Chen, *Nano Energy*, 2015, **17**, 290-301.

15. Y. Liu, S. Yu, R. Feng, A. Bernard, Y. Liu, Y. Zhang, H. Duan, W. Shang, P. Tao, C. Song and T. Deng, *Adv. Mater.*, 2015, **27**, 2768-2774.

16. L. B. Zhang, B. Tang, J. Wu, R. Li and P. Wang, *Adv. Mater.*, 2015, **27**, 4889-4894.

17. H. Ghasemi, G. Ni, A. M. Marconnet, J. Loomis, S. Yerci, N. Miljkovic and G. Chen, *Nat. Commun.*, 2014, **5**, 4449.

18. Y. Zeng, J. Yao, B. A. Horri, K. Wang, Y. Wu, D. Li and H. Wang, *Energy Environ. Sci.*, 2011, **4**, 4074-4078.

View Article Online
DOI: 10.1039/C6NR03921A

19. O. Neumann, A. S. Urban, J. Day, S. Lal, P. Nordlander and N. J. Halas, *ACS Nano*, 2013, **7**, 42-49.

20. R. Jiang, S. Cheng, L. Shao, Q. Ruan and J. Wang, *J. Phys. Chem. C*, 2013, **117**, 8909-8915.

21. D. Jaque, L. M. Maestro, B. del Rosal, P. Haro-Gonzalez, A. Benayas, J. L. Plaza, E. M. Rodríguez and J. García Solé, *Nanoscale*, 2014, **6**, 9494-9530.

22. K. S. Novoselov, A. K. Geim, S. V. Morozov, D. Jiang, Y. Zhang, S. V. Dubonos, I. V. Grigorieva and A. A. Firsov, *Science*, 2004, **306**, 666-669.

23. A. K. Geim and K. S. Novoselov, *Nat. Mater.*, 2007, **6**, 183-191.

24. X. Huang, Z. Zeng, Z. Fan, J. Liu and H. Zhang, *Adv. Mater.*, 2012, **24**, 5979-6004.

25. A. A. Balandin, *Nat. Mater.*, 2011, **10**, 569-581.

26. G. A. Lane, *Solar heat storage: latent heat materials. Background and scientific principles*, vol. 1. CRC Press, Boca Raton, USA 1983.

27. D. Zhou, C. Y. Zhao and Y. Tian, *Applied Energy*, 2012, **92**, 593-605.

28. K. Pielichowska and K. Pielichowski, *Prog. Mater. Sci.*, 2014, **65**, 67-123.

29. H. Ji, D. P. Sellan, M. T. Pettes, X. Kong, J. Ji, L. Shi and R. S. Ruoff, *Energy Environ. Sci.*, 2014, **7**, 1185-1192.

30. I. Kholmanov, J. Kim, E. Ou, R. S. Ruoff and L. Shi, *ACS Nano*, 2015, **9**, 11699-11707.

31. Y. Wang, B. Tang, and S. Zhang, *Adv. Funct. Mater.*, 2013, **23**, 4354–4360.

32. Y. Wang, B. Tang, and S. Zhang, *J. Mater. Chem.*, 2012, **22**, 18145-18150.

33. L. Chen, R. Zou, W. Xia, Z. Liu, Y. Shang, J. Zhu, Y. Wang, J. Lin, D. Xia and A. Cao, *ACS Nano*, 2012, **6**, 10884-10892.

View Article Online
DOI: 10.1039/C6NR03921A

34. L. B. Zhang, G. Chen, M. N Hedhili, H. Zhang and P. Wang, *Nanoscale*, 2012, **4**, 7038-7045.

35. D. Konatham and A. Striolo, *Appl. Phys. Lett.*, 2009, **95**, 163105.

36. Y. Zhong, S. Li, X. Wei, Z. Liu, Q. Guo, J. Shi and L. Liu, *Carbon*, 2010, **48**, 300–304.

Graphical Abstract

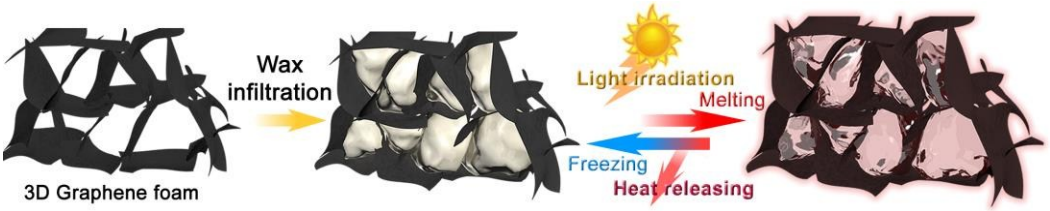

Solar-thermal conversion and thermal storage for sustained energy release are realized by a novel graphene foam and phase-change-material based composite.